High-throughput single-cell transcriptomics data informs mechanisms underlying cell-to-cell differences in stress responses

Authors:
Eder*[1,2], R., Brettner*[1], L., Geiler-Samerotte[1,2], K.
*Co-first authors

Corresponding Author: Kerry Geiler-Samerotte, kerry.samerotte@asu.edu

Affiliations:
[1]Center for Mechanisms of Evolution, Biodesign Institutes, Arizona State University, Tempe, AZ, USA 85287
[2]School of Life Sciences, Arizona State University, Tempe, AZ, USA, 85287

Abstract: Over recent decades, studies of cell-to-cell heterogeneity have shown that meaningful variation in stress responses is an evolved trait, exemplified by bet hedging. Here, we expand upon this work by using a high-throughput single-cell transcriptomics approach in *S. cerevisiae* to study cell-to-cell variation in stress responses. We measured individual transcriptional profiles of over ten thousand cells subjected to two types of stress: protein misfolding (an intrinsic stress) and nutrient deprivation (an extrinsic stress). Doing so, we saw substantial heterogeneity in responses to stress across and within different conditions. A previously defined canonical stress response is elevated in all stressful conditions, making it useful as a barometer of stress. However, it does not include the majority of the genes that are the most upregulated in response to any of the stresses we study, suggesting stress responses vary across environments. On the other hand, the genes that were downregulated with stress show a much stronger overlap across conditions. Even more striking is the cell-to-cell heterogeneity we observed in stress responses where some stressed cells exhibit neither a canonical stress response nor a transcriptional response that matches most other cells in the same vessel. Further investigation of these cell-to-cell differences revealed a misconception of population-averaged data: While transposable elements (TEs) and chaperones both appear positively correlated with stress at the population level, single-cell analysis revealed they are actually anticorrelated. In other words, some stressed cells upregulate TEs, while others upregulate chaperones. One possible mechanism for this involves chaperones, such as Hsp90, which are thought to help to silence TEs but are unable to do so effectively when these chaperones become overwhelmed during stress. In sum, we have used a powerful single-cell transcriptomics approach to quantify stress-response heterogeneity and to shed light on the mechanisms underlying cell-to-cell variation in stress responses, both of which are crucial for understanding cell evolution and disease.

Introduction

Traditional bulk transcriptomics methods have identified common gene expression patterns that occur when microbial cells experience a range of environmental stressors, including changes in the levels of protein-folding chaperones, ribosomes, and metabolic enzymes (Gasch et al. 2000; Brauer et al. 2008; Ho and Gasch 2015). While recent work has surveyed the extent to which stress responses vary across environments and cells, this work is often limited to hundreds of cells (Gasch et al. 2017) and/or a small number of genes (Cai et al. 2008; Munsky et al. 2018; Sampaio et al. 2022; Bergen et al. 2022). Here, we use an emerging ultra-high throughput single-cell transcriptomics method for microbes (Kuchina et al. 2021; Brettner et al. 2024) to study transcriptional responses to multiple different types and levels of stress across 12,488 yeast cells. We expand upon the sets of genes that are typically studied by annotating and including transposable elements (TEs), observing expression levels for a total of 6,641 genes or transcribed regions.

Across all types and levels of stress we study, we see expected transcriptomic changes at the population level, including upregulation of chaperones and downregulation of ribosomes with stress. However, the transcript levels that are the most responsive differ across the stresses we survey and differ from a previously defined canonical stress response in yeast (Gasch et al. 2000; Causton et al. 2001). Perhaps even more striking are the differences we observe from cell to cell. Some cells, despite having sampled many transcripts, show neither a canonical stress response nor a response that looks like most other cells in the same vessel.

Transcriptional differences across single cells exposed to the same environment often reveal insights about the mechanisms that regulate transcription (Cai et al. 2008; Li et al. 2018; Bergen et al. 2022; Kocik and Gasch 2024). For example, previous single-cell work revealed that the expression levels of two key stress-responsive proteins Dot6 and Msn2/4 actually differ across single cells (Bergen et al. 2022) and further demonstrated that one of these (Msn2/4) regulates the other (Kocik and Gasch 2024). Similarly, here we find that the levels of two types of genes that are both upregulated with stress (protein-folding chaperones and TEs) are actually anticorrelated across single cells. A potential mechanism to explain this observation involves chaperones, which can become overwhelmed in some cells, negatively regulating expression of TEs (Specchia et al. 2010; Specchia and Bozzetti 2021). Our findings are set apart from other single-cell work in this field since we capture full transcriptomes, so we do not need to decide *a priori* which stress-response genes to study. This gives us power to discover new interactions between genes and stresses.

Results & Discussion

Protein misfolding provokes the upregulation of unique transcripts.

The first stress we studied was misfolding of a gratuitous cytosolic protein. In order to see whether cells transcriptionally respond to varying levels of misfolding stress in a way that differs from previously-defined stress responses, we utilized strains that express increasingly misfolded variants of yellow fluorescent protein (YFP) (Geiler-Samerotte et al. 2011, 2013). We used three

83 different strains, including a version where very few of the YFPs are misfolded (YFPwt), a
84 version where almost every YFP molecule is misfolded (YFPm4), and a version that falls in
85 between (YFPm3) (***Figure 1A***). As all three strains express YFP from the same promoter type
86 and presumably to the same levels, the only appreciable difference between them should be the
87 fraction of YFP that misfolds.
88
89 To determine if cells elicit a transcriptional response to misfolding stress, we measured the
90 percent of the transcriptome that cells devote to a canonical stress response in yeast known as
91 the induced Environmental Stress Response (iESR) (Gasch et al. 2000). As expected, the
92 median proportion of transcripts per cell devoted to the iESR increases from YFPwt to YFPm4
93 (***Figure 1B***). However, despite the misfolded protein burden, not to mention the shared burden
94 of overexpressing YFPs, the percent of the detected transcriptome dedicated to the iESR is
95 relatively small in all strains, only up to ~10% (***Figure 1B***).
96
97 We next determined the genes that were significantly upregulated in our misfolded protein strain
98 (YFPm4) compared to the wildtype strain (YFPwt). In our data, we detected 124 genes that
99 comprise our induced misfolded protein stress response (iMSR). Surprisingly, only 5 of these
100 genes overlap with the iESR (***Figure 1C***). The iMSR comprises up to 30% of the transcriptome
101 of each cell and, on average, increases from YFPwt to YFPm3 to YFPm4 (***Figure 1D***). Thirty-six
102 of the iMSR genes are TEs, which are often not included in microarrays such as those used to
103 define the iESR (Gasch et al. 2000). Other unique prominent gene ontology (GO) terms
104 associated with the iMSR were metal iron transport and lysine synthetic pathways, which have
105 been previously shown to be upregulated with misfolding stress (Fernandez et al. 2003).
106
107 **Nutrient deprivation also provokes distinct transcriptional responses.**
108 To test the effects of an external stressor, we compared batch cultured cells from low stress
109 (early in growth when cells are replete with nutrients) to high stress (late term growth when cells
110 are becoming starved and surrounded by toxic metabolites) (***Figure 1E***). We have data for five
111 different yeast strains in two different types of carbon-limited media, glucose (two of the strains)
112 and sucrose/raffinose (three of the strains) (***Figure 1E***). Again as with misfolded protein stress,
113 the percentage of the transcriptome devoted to the iESR increases over time as cells deplete
114 their nutrients (***Figure 1F***). These combined results (***Figure 1B*** and ***1F)*** confirm the utility of the
115 iESR as a barometer for stress, as have many previous studies (Gasch et al. 2000, 2017;
116 Causton et al. 2001; Brauer et al. 2008).
117
118 However, if we perform the same analysis to determine the induced nutrient stress responses in
119 glucose and sucrose/raffinose (iNSRg and iNSRs, respectively), we see a similar disjoint
120 between the genes detected in the iESR, and with each other, with only 7 genes appearing in all
121 three defined responses (***Figure 1G***). Both the iNSRg and iNSRs comprise an upregulation of
122 TEs, as does the iMSR. But the iNSRg uniquely comprises genes relating to the endoplasmic
123 reticulum (ER) stress response as well as mitochondrial protein degradation. On the other hand,
124 the iNSRs uniquely comprises Ub-specific processing proteases (UBPs) and actin cytoskeleton
125 organization. These stress responses reach high levels, up to 60% of the transcriptome of each
126 cell when nutrient deprivation is at its highest (***Figure 1H***).

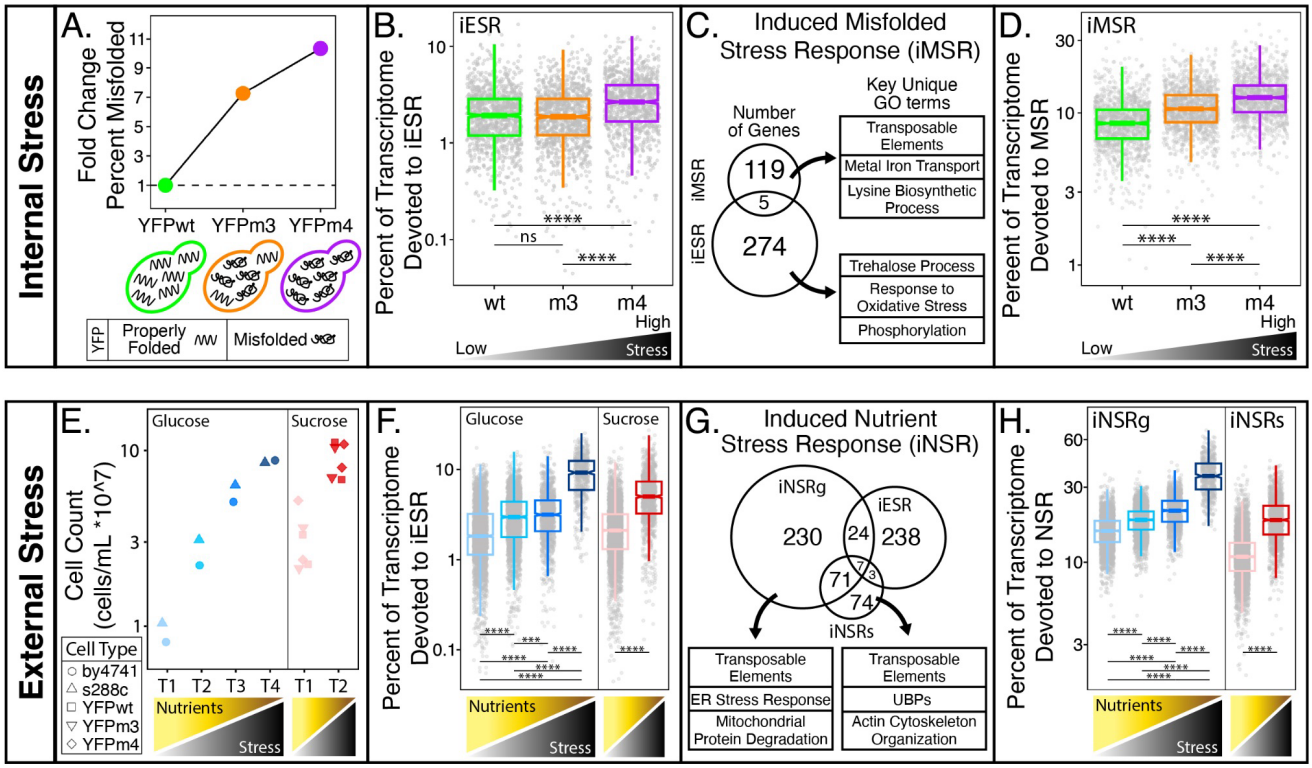

Figure 1: Transcriptional responses differ across degree and type of stressors. **Top row: misfolded protein stress (internal) A.** Protein misfolding, as measured by the percent insoluble fraction, increases with mutation type relative to wildtype (Geiler-Samerotte et al. 2011). YFPm3 has approximately 7-fold more misfolded protein than YFPwt, and YFPm4 has approximately 11-fold more than YFPwt. Note that the total amount of YFP expressed in each strain has been shown to be constant (Geiler-Samerotte et al. 2011). **B.** The percent of the transcriptome devoted to the iESR increases with misfolding stress. Median and quartiles are shown for cell data from two replicates per strain sampled in early log-linear growth. Cells with no detected iESR gene transcripts were excluded. P-values calculated using a t-test, **** indicates $p < 0.0001$, ns indicates nonsignificant. **C.** Venn diagram showing only a small degree of overlap in the defining genes for the iESR and iMSR. Three unique GO terms from each response are listed. **D.** The same as in B but for the iMSR genes. **Bottom row: nutrient stress (external) E.** Yeast strains (indicated by symbol) were sampled in replicate from 4 timepoints in glucose-limited media (blue) and two timepoints in sucrose/raffinose-limited media (red) with an assumed decrease in nutrients and increase in stress with increased time and cell density. **F, G,** and **H.** The same as in **B, C,** and **D** but nutrient stress conditions (glucose**:** blue**/**iNSRg**,** sucrose/raffinose**:** red/iNSRs). P-value of *** indicates $p < 0.001$.

146 **Induced transcripts are more unique to the stressor than repressed transcripts.**
147 As demonstrated in **Figure 1C** and **1G**, the transcriptional response to stress—specifically, the
148 upregulation of certain genes—varies considerably across different stressors. We next
149 investigated whether the set of genes downregulated in response to internal or external stress
150 exhibits a similar degree of variability. Our findings indicate that these genes comprising the
151 repressed stress responses do not (Figure 2). Genes repressed under stress conditions
152 predominantly include those associated with cellular growth processes, such as ribosomal
153 biogenesis (Gasch et al., 2000; Brauer et al., 2008). Although a greater number of genes exhibit
154 significant downregulation in response to stress, fewer *unique* genes define the repressed
155 response in each specific environment. In other words, while each stress-induced transcriptional
156 response is characterized by a large number of uniquely upregulated transcripts (***Figure 2;***
157 black bars), the downregulated genes exhibit greater conservation across different stress
158 conditions, with fewer transcripts uniquely repressed in a stress-specific manner (***Figure 2;***
159 yellow bars).
160

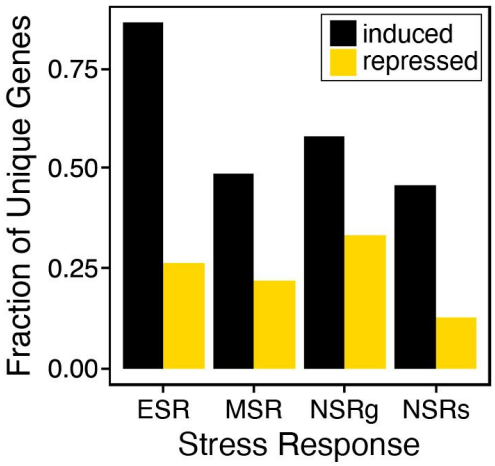

161
162 ***Figure 2: The transcripts induced in response to stress differ more across environments***
163 ***than the transcripts that are repressed.*** Each bar displays the fraction of unique genes, or the
164 fraction of genes that are found in no other stress response except the one in which it
165 originates, that are included in either an induced (black) or repressed (yellow) stress response.
166
167 **Not all cells expressing misfolded proteins manifest a defined stress response.**
168 In addition to transcriptional stress response variation across different environmental stress
169 conditions, we also observe significant heterogeneity at the single-cell level. This is evident in
170 ***Figure 1B, 1D, 1F,*** and ***1H,*** where each point represents an individual cell, and the dispersion
171 of points along the vertical axis reflects variability in the percent of each cell's transcriptome
172 dedicated to the stress response. Similar variation is observed in ***Figure 3A,*** which further
173 demonstrates an inverse correlation between the percent of a cell's transcriptome allocated to
174 the induced Environmental Stress Response (iESR) (***Figure 3A;*** bars) and that allocated to the
175 repressed Environmental Stress Response (rESR) (***Figure 3A;*** points). While the majority of
176 YFPm4-expressing cells exhibit a higher abundance of iESR transcripts compared to YFPwt-
177 expressing cells (***Figures 1B*** and ***3A***), some cells deviate from this trend. Notably, among the
178 10% of cells with the lowest iESR expression, a substantial fraction consists of YFPm4-

expressing cells (***Figure 3A;*** left). This pattern persists at a less drastic level when also analyzing the iMSR (***Figure 3A;*** right).

These results highlight a potential danger in assuming one can predict a cell's intrinsic or extrinsic condition solely from its transcriptome. It is unclear whether the variation we see in single-cell transcriptional responses is simply noise, whereby some cells fail to reach the optimum transcriptional state in a given environment, or whether this variation is a meaningful feature of cell populations that allows cells to diversify and survive environmental fluctuations (e.g., a bet hedging mechanism) (Levy et al. 2012). What is clear is that this noise is not an artifact of our study system; a similar result was observed in a study surveying fewer cells with more transcripts per cell (Gasch et al. 2017).

Not all cells experiencing nutrient deprivation manifest a defined stress response.
To determine whether similar variation exists in cell-to-cell responses to nutrient exhaustion, we compared cells sampled at the earliest time point (***Figure 1E;*** T1 in glucose, light blue) to those sampled approximately six hours later, after cell density had increased approximately 6-fold and nutrients were largely depleted (***Figure 1E;*** T3 in glucose, dark blue). Regardless of whether we examine the induced Environmental Stress Response (iESR) or the induced Nutrient Stress Response (iNSRg), a cell's transcriptome does not wholly distinguish between T1 and T3 (***Figure 3B***). Notably, some cells sampled at high density and under nutrient-depleted conditions exhibit transcriptomic profiles similar to those of cells sampled at lower density and in nutrient-rich conditions, in terms of both induced (bars) and repressed (points) stress responses (***Figure 3B***). This pattern persists across similar comparisons, such as between early and late-sampled cells in sucrose/raffinose-limited media (data not shown).

However, cell-to-cell variation in the iESR decreases as stress severity increases (***Figure 3C;*** top), suggesting that under more extreme conditions, a greater proportion of cells exhibit a transcriptional response more consistent with the expected stress adaptation. In contrast, the repressed environmental stress response (rESR) (consisting of growth responses) exhibits the opposite pattern, becoming more variable as stress severity increases, suggesting the degree of stress as an environmental driver of the observed transcriptional variation between cells (***Figure 3C;*** bottom).

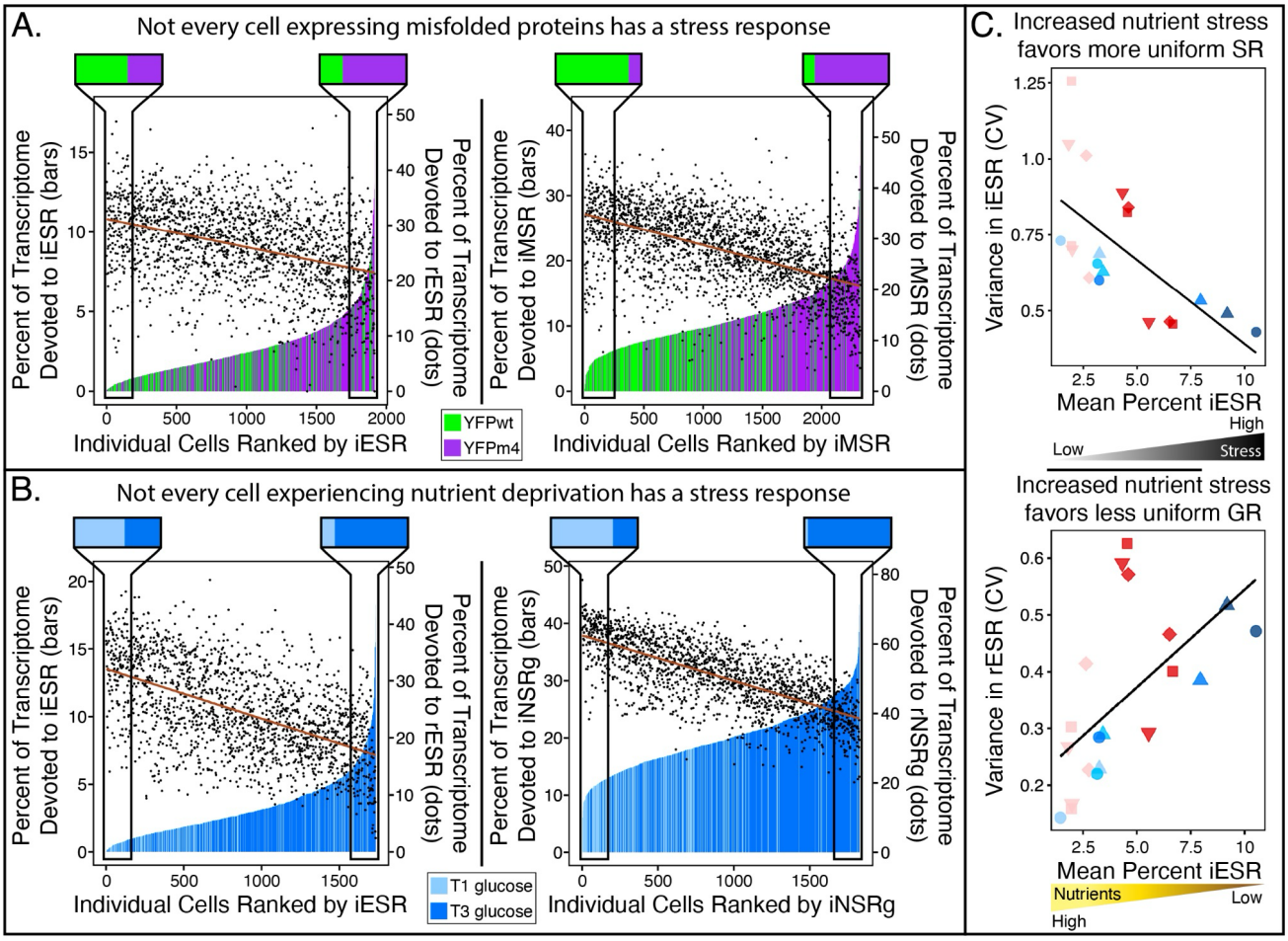

Figure 3: Single-cell heterogeneity in the expression of transcriptional stress response. **A.** YFPwt and YFPm4 cells are ordered by their percent transcriptome dedicated to the iESR (bars, left) or iMSR (bars, right). An inverse correlation is observed between the percent iESR expressed and percent rESR (points, fit line). Fractional bar scales indicate the proportion of the bottom and top 10% of cells expressing the iESR or iMSR demonstrating cell type non-uniformity in both categories. **B.** The same as in A, but for T1 and T3 cells grown in glucose-limited media (see Figure 1). **C. Top:** iESR expression variation, as measured by the population coefficient of variation (CV), decreases as the population mean iESR expression increases. Data colors and symbols are the same as in ***Figure 1E***. 'SR' stands for 'stress response'. **Bottom:** rESR expression variation (CV) increases with population mean iESR expression. 'GR' stands for 'growth response'.

Some cells express neither an iESR nor an rESR.

In ***Figure 3A*** and ***3B,*** we see an anticorrelation of the induced and repressed stress responses consistent with previous studies (Gasch et al. 2000). Some have even suggested the iESR is not a specific response to stress but merely represents transcriptional changes that take place when cells slow their growth rates (Brauer et al. 2008). A view that emerges from previous work is that, to some degree, the transcriptome can be thought of as a speedometer, because large

232 sets of transcripts adjust their levels in lock step with cell growth rate. However, using high-
233 throughput single-cell RNAseq, we and others (Ho et al. 2018; Li et al. 2018) can see that this
234 view misses important subpopulations of cells where growth rate and stress-responsive
235 transcript levels are uncoupled.
236
237 Specifically, when we look at all of the cells sampled from one of our most stressful conditions
238 (T4 in ***Figure 1E***), we see that most cells fall into a subpopulation that upregulates the iESR, as
239 expected (***Figure 4A***; cluster 2 in left panel). However, a second subpopulation of cells, with
240 distinct transcriptional signatures as defined by the Louvain clustering algorithm, does not
241 appear to be expressing high levels of the iESR, even though all of these cells are from the
242 same stressful condition (***Figure 4A***; cluster 1 in left panel). If we did not have high-throughput
243 single-cell data and only the population average or a small number of cells was used to
244 investigate the iESR, this interesting but small subpopulation of cells that do not manifest the
245 iESR would be undetectable.
246
247 Since these cells in cluster 1 have relatively low levels of the iESR, one might assume that they
248 have relatively high levels of the rESR, since these responses appear to be anticorrelated in
249 ours and others work (Gasch et al. 2000). Yet we do not observe substantial upregulation of the
250 rESR in cluster 1 cells (***FIgure 4A***; middle panel). Further, in most cluster 1 cells, the iESR plus
251 rESR comprises less than 20% of the transcriptome. This begs the question, What genes are
252 being expressed in these cluster 1 cells? We further investigated gene sets and determined that
253 cluster 1 is highly enriched for TEs, meaning that a much higher percent of these cells'
254 transcriptomes are devoted to TEs, rather than either the iESR or rESR (***Figure 4A***; right
255 panel). Overall, our work uses single-cell transcriptomics to reveal that the mechanisms
256 regulating transcription appear to be more complex than a simple lever that tips each cell's
257 transcriptomes towards a fast or slow growth modality.
258
259 **While the iESR and TEs increase with stress, they are anticorrelated at the single-cell**
260 **level.**
261 As an example of how single-cell data are useful in understanding the mechanisms regulating
262 transcription, here we present the test case of TEs. Very similarly to the iESR, the fraction of the
263 transcriptome composed of TEs increases with all stressors that we study, such that the
264 average levels of TEs and the iESR are positively correlated (***Figure 4B***). This might easily lead
265 to the false assumption that stressed cells possess *both* more TEs and higher levels of iESR
266 transcripts. However, this is not true. At the single-cell level, TEs and the iESR are negatively
267 correlated (***Figure 4C***). Cells that have high levels of TEs have low levels of iESR transcripts
268 and vice versa. This negative correlation is true of nearly every sample of single cells that we
269 collected, regardless of strain background or stress level (***Figure 4D;*** all points in the teal
270 boxplots are near or below zero and thus tend to describe negative correlations). These
271 negative correlations are not artifacts of our method and, in fact, might be even stronger in
272 reality given the sparsity of single-cell RNA sequencing data which tends to minimize detectable
273 correlations. Additionally, when we randomly divide the iESR or iMSR in two and calculate the
274 correlation between each half across single cells, we see positive correlations (***Figure 4D;*** all
275 points in the gray boxplots are above zero).

A proposed mechanism explaining the anticorrelation between the iESR and TEs.

The iESR comprises a large number of protein-folding chaperones, which have been shown to be upregulated with stress in organisms across the tree of life (Lindquist and Craig 1988). Previous work suggests that a particular chaperone (Hsp90) negatively regulates TEs. Specifically, Hsp90 stabilizes Sir2, a histone deacetylase (Huang et al. 2007; Laskar et al. 2011; Khurana and Bhattacharyya 2015), which, in its active form, converts euchromatin to heterochromatin. It is known that TEs are enriched in heterochromatin regions, making Sir2 act as a gene silencing mechanism by putting chromatin in a dense state that is less accessible by RNA polymerase (Di Stefano 2022). Here, we propose a novel mechanism whereby misfolded protein stress overwhelms Hsp90's ability to silence TEs in some cells. In stressful conditions resulting in higher levels of an iESR response, Hsp90 can become overwhelmed, decreasing levels of free Hsp90, which in turn decreases active Sir2. This results in TEs being more readily available to be transcribed on loose euchromatin, explaining why we found an anticorrelation between the iESR and TEs as well as chaperones and TEs (***Figure 4D***) on the single-cell level. Similar mechanisms are defined in other organisms with piRNA, or PIWI-interacting RNA, that interact with chromatin modifying, stem and germ cell differentiation, and are essential to silence TEs (Brennecke et al. 2007; Ghildiyal and Zamore 2009). In a similar fashion to yeast Sir2, Hsp90 also stabilizes PIWI proteins. Recent work has questioned the implication of TEs in aging related diseases (Wood and Helfand 2013), such as with Alzheimer's Disease (Feng et al. 2025), and further studies on misfolding could explore whether the misfolded proteins themselves are toxic to cells or if downstream implications of chaperone machinery availability (i.e., TEs) could be a greater culprit than suspected. A key point is that this negative regulation of TEs by chaperones was only revealed because we have high-throughput single-cell transcriptomics data. Without it, we may have assumed TEs and chaperones are concomitantly upregulated by stress (***Figure 4E***).

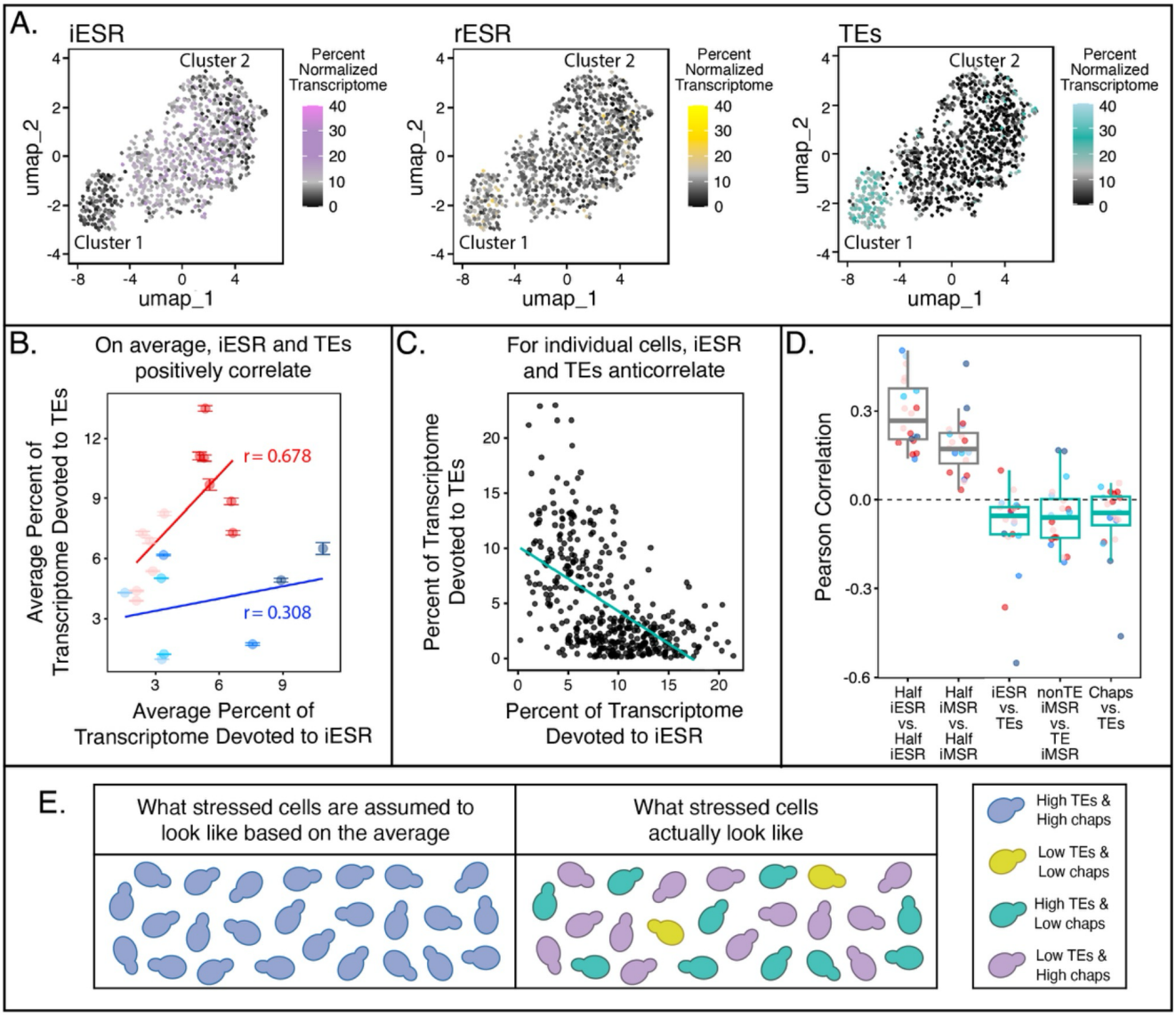

Figure 4: Anticorrelation of TEs and iESR expression on single-cell level. **A.** Two distinct clusters, or subpopulations, of cells from bin T4 in glucose-limited growth were found by using a Louvain clustering analysis that determines how closely related each cell's transcriptome is to all other cells. UMAPs were generated for visualization purposes. The plots are colored by the percent normalized transcriptome for iESR, rESR, and TE gene sets. **B.** The average percent of the transcriptome devoted to the iESR versus TEs is plotted for each sample. Points are colored the same as ***Figure 1E.*** Error bars display the standard error of the mean across replicate experiments. Pearson correlations are provided and show a positive correlation between the iESR and TEs on the population level. **C.** Looking at just a single yeast strain (s288c) in T4 in glucose-limited growth, we plotted the correlation between the percent of the transcriptome devoted to the iESR versus TEs for individual cells (with each point representing an individual cell). On the single-cell level, the iESR and TEs anticorrelate. **D.** TEs and the iESR anticorrelate across single cells in many other strains and environments. Pearson correlations between

317 different gene sets are shown for all 20 conditions colored the same as ***Figure 1E***. **E.** A
318 schematic example shows a misconception of population-averaged data where stressed cells
319 may be assumed to have high TEs and high chaperones based on the results of ***Figure 4B***
320 when, actually, they have either one or the other (based on the results of ***Figures 4C*** and ***4D***).
321
322 **Methods**
323
324 **Experimental Methods**
325
326 **Yeast strains**
327 *Saccharomyces cerevisiae* strain *MATa ura3A0 his3Δ 1 met17Δ 0 P ACT1-GAL3::SpHIS5*
328 *gal11Δ gal10Δ ::LEU2 leu2Δ 0::P GAL1 -YFP-KanMX6 ybr209wΔ ::BC3-HphMX6* with wildtype,
329 m3, and m4 YFP mutations were used for intrinsic misfolding and extrinsic nutrient deprivation
330 stress experiments in sucrose/raffinose-limited media ((Geiler-Samerotte et al. 2011)). We also
331 used diploid s288c and a genetically naive haploid BY4741 for glucose nutrient deprivation
332 experiments.

333 **Yeast cell culture**
334 Cells were streaked on YP plus 2% dextrose agar plates from frozen -80C glycerol stocks and
335 grown at 30C for 48 hours. Colonies were then picked into liquid YP plus 2% dextrose and
336 grown at 30C with shaking overnight. The YFP strains were diluted into Synthetic Complete
337 minus glucose (Sunrise) plus 2.5% sucrose, 1.25% raffinose, and 0.625% galactose media to
338 induce YFP expression. Diploid s288c cells and haploid BY4741 cells were diluted into
339 Synthetic Complete (Sunrise) plus 2% glucose media. All cultures were massively diluted by
340 measuring the overnight culture density and adding approximately 15,000 total cells to 50 mL of
341 media (300 cells/mL). These cultures were then subsequently grown at 30C with shaking, and
342 sampled and measured systematically until the populations started to enter stationary phase.
343 The samples were saved and processed for single-cell RNA sequencing using the SPLiT-seq
344 method.
345
346 **Single-cell RNA sequencing**
347 Single-cell RNA sequencing was performed using a yeast-specific application of split-pool
348 based *in situ* transcriptomics sequencing (SPLiT-seq) as previously described in (Brettner et al.
349 2024).
350
351 **Data Analysis Methods**
352
353 **Single-cell RNA seq data processing**
354 Transcriptome alignment, barcode assignment, and gene expression count analyses were
355 performed as described in (Brettner et al. 2024). Briefly, sequencing reads were aligned to the
356 R64 s288c genome from NCBI supplemented with transposon sequences from the
357 Saccharomyces Genome Database and sorted by barcode using STARsolo (Dobin et al. 2013).
358 As the yeast genome has significant sequence homology, especially between rRNA genes, we
359 enabled the uniform multimapping algorithm within STARsolo to keep overlapping reads. This
360 outputted gene-by-barcode matrices representing the detected gene counts for every cell. To
361 remove empty and low gene detection barcodes, we applied the “knee” detection filter
362 previously described in (Brettner et al. 2024). These quality-thresholded gene-by-barcode
363 matrices were then converted to the R datatype Seurat Objects using the Seurat R package for
364 further analyses (Hao et al. 2024). rRNA genes were identified and removed so they would not
365 distort subsequent calculations and analyses. Normalization, scaling, nearest neighbor

366 calculations, clustering, and differential expression analyses were performed similar to the
367 tutorial provided by the Satija Lab (Hao et al. 2024) on mRNA datasets with the rRNA removed.
368
369 **Single-cell data analysis**
370
371 **Calculating percent of transcriptome devoted to different gene sets**
372 The Seurat Object with all data was converted to a large matrix and then a dataframe for easier
373 manipulation in R. As each row is a single cell defined by its barcode and each column is a
374 gene, we took row sums to determine the total number of gene counts per cell, giving us all
375 counts for a cell. For each gene set, we subsetted the overall dataframe to only include the
376 desired genes for one gene set at a time. Row sums for those subsets were taken. To
377 determine the percent of the transcriptome devoted to each gene set, we then divided our
378 subsetted counts by the all counts for each individual cell. For the half iESR versus half iESR
379 and half iMSR versus half iMSR calculations (***Figure 4D***), a random sample without
380 replacement to split the lists in half was taken.
381
382 **Creating induced and repressed stress response gene lists**
383 To determine the induced and repressed stress response genes, we compared gene expression
384 of cells in the early log YFPwt versus YFPm4 (MSR), YFPwt early log vs YFPwt late log (NSRs),
385 and T1 vs T4 (NSRg). We used a pseudo-bulk analysis for each of the groups being compared.
386 This consisted of summing genes across all cells in a given condition and dividing by the total
387 detected read counts. These ratios were converted to transcripts per million by multiplying by
388 10^6. Log2 ratios were calculated for each comparison to generate a fold change. P-values
389 were calculated by performing a nonparametric Wilcoxon signed-rank test of by-cell expression
390 of genes between each comparisons and then multiple-comparison corrected using a Bonferroni
391 p-value adjustment. Genes with a corrected significance of $p < 0.05$ were kept as part of the
392 induced or repressed stress responses depending on the direction of their fold change.
393
394 **Removing low counts**
395 For each gene set percent calculation, we removed the cells expressing the lowest 10% of
396 all/total counts from each experiment (three in total: two for the YFPs and one for s288c and
397 by4741 (done on the same day as experiment two of the YFPs)).
398
399 **Densities**
400 The cell densities were recorded as described above during sampling. Densities were averaged
401 for replicates of the same cell type sampled in the same timepoint.
402
403 **Comparing equal number of cells in bar/dot plots (*Figure 3A* and *3B*)**
404 For each graph, an equal number of cells from each cell type/timepoint being plotted together
405 were taken. Based on the group with the lowest number of cells in the comparison, we randomly
406 sampled an equal number from the other group.
407
408 **Coefficient of Variance**
409 CV was calculated for each group based on the 20 possible sampletime, celltype, and
410 experiment combinations. The standard deviation of the mean of all gene counts (CountsNorm)
411 was divided by the mean of all gene counts (CountsNorm).
412
413 **Removing zeros for plotting purposes**
414 For boxplots (***Figure 1B, 1D, 1F,*** and 1***H***), any cells that had zero percent of their transcriptome
415 devoted to the stress category being plotted were excluded for a given plot. Due to the sparse
416 nature of single-cell data, these cells with zero reads may actually have none of the stress

response, or these reads may just not have been found. These cells with zeros were also excluded from ***Figure 3A*** and **3D**. This resulted in ***Figure 1B*** having a total of 1165 YFPwt, 1170 YFPm3, and 1082 YFPm4 cells. ***Figure 1D*** has a total of 1340 YFPwt, 1341 YFPm3, and 1218 YFPm4. ***Figure 1F*** has 2744 T1, 2468 T2, 1213 T3, and 541 T4 cells per bin for glucose-limited media and a total of 3417 T1 and 1175 T2 cells per bin for sucrose/raffinose-limited media. ***Figure 1H*** has a total of 2892 T1, 2551 T2, 1261 T3, and 541 T4 cells per bin for glucose-limited media and a total of 3898 T1 and 1342 T2 cells per bin for sucrose/raffinose-limited media.

Removing outliers for plotting purposes

A few outliers were removed on plots to help axes not be as stretched. In ***Figure 1H,*** the 3 lowest outliers were removed. In ***Figure 3A*** for the iMSR, the cell with the highest percent of its transcriptome devoted to the iMSR was removed.

Gene ontology analysis

Simple gene ontology analyses were done by manually entering genes into both Metascape and SGD (Cherry et al. 2012; Zhou et al. 2019)

References

Bergen AC, Kocik RA, Hose J, et al (2022) Modeling single-cell phenotypes links yeast stress acclimation to transcriptional repression and pre-stress cellular states. Elife 11.: https://doi.org/10.7554/eLife.82017

Brauer MJ, Huttenhower C, Airoldi EM, et al (2008) Coordination of Growth Rate, Cell Cycle, Stress Response, and Metabolic Activity in Yeast. Molecular Biology of the Cell 19:352–367

Brennecke J, Aravin AA, Stark A, et al (2007) Discrete small RNA-generating loci as master regulators of transposon activity in Drosophila. Cell 128:1089–1103

Brettner L, Eder R, Schmidlin K, Geiler-Samerotte K (2024) An ultra high-throughput, massively multiplexable, single-cell RNA-seq platform in yeasts. Yeast

Cai L, Dalal CK, Elowitz MB (2008) Frequency-modulated nuclear localization bursts coordinate gene regulation. Nature 455:485–490

Causton HC, Ren B, Koh SS, et al (2001) Remodeling of yeast genome expression in response to environmental changes. Mol Biol Cell 12:323–337

Cherry JM, Hong EL, Amundsen C, et al (2012) Saccharomyces Genome Database: the genomics resource of budding yeast. Nucleic Acids Res 40:D700–5

Di Stefano L (2022) All quiet on the TE front? The role of chromatin in transposable element silencing. Cells 11:2501

Dobin A, Davis CA, Schlesinger F, et al (2013) STAR: ultrafast universal RNA-seq aligner. Bioinformatics 29:15–21

Feng Y, Cao S-Q, Shi Y, et al (2025) Human herpesvirus-associated transposable element activation in human aging brains with Alzheimer's disease. Alzheimers Dement 21:e14595

Fernandez J, Lopez AB, Wang C, et al (2003) Transcriptional control of the arginine/lysine

458 transporter, cat-1, by physiological stress. J Biol Chem 278:50000–50009

459 Gasch AP, Spellman PT, Kao CM, et al (2000) Genomic expression programs in the response
460 of yeast cells to environmental changes. Mol Biol Cell 11:4241–4257

461 Gasch AP, Yu FB, Hose J, et al (2017) Single-cell RNA sequencing reveals intrinsic and
462 extrinsic regulatory heterogeneity in yeast responding to stress. PLoS Biol 15:e2004050

463 Geiler-Samerotte KA, Dion MF, Budnik BA, et al (2011) Misfolded proteins impose a dosage-
464 dependent fitness cost and trigger a cytosolic unfolded protein response in yeast.
465 Proceedings of the National Academy of Sciences 108:680–685

466 Geiler-Samerotte KA, Hashimoto T, Dion MF, et al (2013) Quantifying condition-dependent
467 intracellular protein levels enables high-precision fitness estimates. PLoS One 8:e75320

468 Ghildiyal M, Zamore PD (2009) Small silencing RNAs: an expanding universe. Nat Rev Genet
469 10:94–108

470 Hao Y, Stuart T, Kowalski MH, et al (2024) Dictionary learning for integrative, multimodal and
471 scalable single-cell analysis. Nat Biotechnol 42:293–304

472 Ho Y-H, Gasch AP (2015) Exploiting the yeast stress-activated signaling network to inform on
473 stress biology and disease signaling. Curr Genet 61:503–511

474 Ho Y-H, Shishkova E, Hose J, et al (2018) Decoupling yeast cell division and stress defense
475 implicates mRNA repression in translational reallocation during stress. Curr Biol 28:2673–
476 2680.e4

477 Huang L, Sun Q, Qin F, et al (2007) Down-regulation of a SILENT INFORMATION
478 REGULATOR2-related histone deacetylase gene, OsSRT1, induces DNA fragmentation
479 and cell death in rice. Plant Physiol 144:1508–1519

480 Khurana N, Bhattacharyya S (2015) Hsp90, the concertmaster: tuning transcription. Front Oncol
481 5:100

482 Kocik RA, Gasch AP (2024) Regulated resource reallocation is transcriptionally hard wired into
483 the yeast stress response. bioRxivorg

484 Kuchina A, Brettner LM, Paleologu L, et al (2021) Microbial single-cell RNA sequencing by split-
485 pool barcoding. Science 371.: https://doi.org/10.1126/science.aba5257

486 Laskar S, Bhattacharyya MK, Shankar R, Bhattacharyya S (2011) HSP90 controls SIR2
487 mediated gene silencing. PLoS One 6:e23406

488 Levy SF, Ziv N, Siegal ML (2012) Bet hedging in yeast by heterogeneous, age-correlated
489 expression of a stress protectant. PLoS Biol 10:e1001325

490 Lindquist S, Craig EA (1988) THE HEAT-SHOCK PROTEINS. Annu Rev Genet 22:631–677

491 Li S, Giardina DM, Siegal ML (2018) Control of nongenetic heterogeneity in growth rate and
492 stress tolerance of Saccharomyces cerevisiae by cyclic AMP-regulated transcription
493 factors. PLoS Genet 14:e1007744

494 Munsky B, Li G, Fox ZR, et al (2018) Distribution shapes govern the discovery of predictive
495 models for gene regulation. Proc Natl Acad Sci U S A 115:7533–7538

496 Sampaio NMV, Blassick CM, Andreani V, et al (2022) Dynamic gene expression and growth
497 underlie cell-to-cell heterogeneity in Escherichia coli stress response. Proc Natl Acad Sci U
498 S A 119:e2115032119

499 Specchia V, Bozzetti MP (2021) The role of HSP90 in preserving the integrity of genomes
500 against transposons is evolutionarily conserved. Cells 10:1096

501 Specchia V, Piacentini L, Tritto P, et al (2010) Hsp90 prevents phenotypic variation by
502 suppressing the mutagenic activity of transposons. Nature 463:662–665

503 Wood JG, Helfand SL (2013) Chromatin structure and transposable elements in organismal
504 aging. Front Genet 4:274

505 Zhou Y, Zhou B, Pache L, et al (2019) Metascape provides a biologist-oriented resource for the
506 analysis of systems-level datasets. Nat Commun 10:1523

507